Estuarine, Coastal and Shelf Science 198 (2017) 128–137

Contents lists available at ScienceDirect

Estuarine, Coastal and Shelf Science

journal homepage: www.elsevier.com/locate/ecss

# Submarine groundwater discharge within a landslide scar at the French Mediterranean coast

Till Oehler [a, *], José M. Mogollón [b], Nils Moosdorf [a], Andreas Winkler [c], Achim Kopf [d], Thomas Pichler [e]

[a] Leibniz Centre for Tropical Marine Research (ZMT), Fahrenheitstraße 6, 28359 Bremen, Germany
[b] Department of Earth Sciences – Geochemistry, Princetonplein 9, 3584CC Utrecht, The Netherlands
[c] Freie Universität Berlin - Fachbereich Geowissenschaften, Malteserstr. 74 – 100, D 12249 Berlin, Germany
[d] MARUM, Dept. of Geosciences, Leobener Str., 28359 Bremen Germany
[e] University of Bremen, Department of Geosciences GEO I, Klagenfurter Str. 4, 28359 Bremen Germany

ARTICLE INFO

*Article history:*
Received 29 July 2016
Received in revised form
6 September 2017
Accepted 8 September 2017
Available online 9 September 2017

*Keywords:*
Submarine groundwater discharge
Subterranean estuary
Mediterranean Sea
Pore water
Barium

ABSTRACT

Submarine groundwater discharge (SGD), the flow of fresh and saline groundwater from the seabed into the coastal ocean, has been intensively investigated in the recent years. This research has usually been restricted to shallow water and intertidal areas, whereas knowledge about groundwater seepage in deeper water is mainly limited to point sources from karstic aquifers. In this study we observed submarine groundwater seepage and a subterranean estuary in sediments at water depths of 20–44 m located within the Ligurian Margin, western Mediterranean Sea. Here, a catastrophic submarine landslide occurred near the Nice airport (French Ligurian coast) in the fall of 1979 after a period of heavy rainfall. During two research cruises, gravity cores were recovered in and around the area of the landslide scar. Pore water samples collected from sediment cores indicated sediments containing freshwater within the landslide scar. Pore water profiles of selected ions, such as chloride, ammonium, manganese, sulfate and barium were used to assess transport and reaction processes within the sediment. A 1-dimensional transport model indicates in most cores upward pore water velocities of 2.3–8.8 cm $yr^{-1}$. This study shows that submarine groundwater seepage along the French Mediterranean coastline can occur at water depths reaching 44 m.



## 1. Introduction

Submarine groundwater discharge (SGD) refers to any water mass discharging from the seabed to the ocean, including terrestrial fresh and recirculated saline water (Burnett et al., 2003). SGD is driven by a variety of factors including tides, waves, bottom currents, and/or density driven transport processes (Burnett et al., 2006; Santos et al., 2009). The mixing of freshwater and seawater leads to a variety of chemical reactions in the "subterranean estuary" (STE) (Moore, 1999).

The distribution of inert and reactive solutes within marine sediments can elucidate transport and reaction processes within the STE. Chloride, a chemically inert species, can be used as a tracer to study the distribution of fresh groundwater and seawater within marine sediments. The pore water concentration profile of chloride may be used to model advective and diffusive freshwater discharge from marine sediments into the sea (Berner, 1980; Schlüter et al., 2004). Reactive solutes may also be used to trace the distribution of seawater within the STE. However, they may be subject to biogeochemical alterations according to the sedimentary redox dynamics. For example, ammonium is typically released during the degradation of organic matter but may be oxidized during nitrification in the presence of oxygen (Froelich et al., 1979; Mogollón et al., 2016). Likewise, barium can be released into the pore water from the dissolution of minerals (e.g barite, Mn oxides), or desorption from particles when fresh groundwater and seawater are mixed (Froelich et al., 1979; Charette and Sholkovitz, 2006; Santos et al., 2011; Russak et al., 2016) and has been associated with SGD occurrence e.g. in the Ganges-Brahmaputra delta (Moore, 1997).

* Corresponding author.
*E-mail addresses:* Till.Oehler@zmt-bremen.de (T. Oehler), J.M.MogollonLee@uu.nl (J.M. Mogollón), nils_sci@moosdorf.de (N. Moosdorf), rnlab@zedat.fu-berlin.de (A. Winkler), akopf@marum.de (A. Kopf), Pichler@uni-bremen.de (T. Pichler).

http://dx.doi.org/10.1016/j.ecss.2017.09.006
0272-7714/

SGD, in the form of submarine springs, is a common feature of the Mediterranean coast (Fleury et al., 2007), including locations in Turkey (Elhatip, 2003), Greece (Tsabaris et al., 2011), Italy (Povinec et al., 2006), France (Dörflinger, 2003), and Spain (Garcia-Solsona et al., 2010b). These springs have been used as freshwater source for at least 2000 years and some are still used today (Gilli, 2015). SGD was shown to transport substantial amounts of nutrients to the Mediterranean (Rodellas et al., 2015), which could lead to eutrophication in coastal ecosystems. Most of the studies of submarine groundwater discharge in the Mediterranean have focused on submarine springs from karstic aquifers, but SGD from sediments could also have a strong effect on coastal environments.

In 1979 a submarine landslide was triggered south of the airport of Nice (France), which exposed freshwater-charged sediments to seawater (Kopf et al., 2010) and thus created an ideal research location for SGD. The landslide was hypothesized to be triggered by groundwater charging into weak, clay-mineral rich layers in the alluvial fan, which had been gradually destabilized by anthropogenic activity on the shelf (Stegmann et al., 2011). This study investigates the current status of SGD within the Nice airport landslide scar by evaluating 13 profiles taken from an STE located in water depths of down to 44 m.

## 2. Study area

The study area is located in the Ligurian Sea (French Mediterranean coast), close to the Var river mouth and the Nice Côte d'Azur airport (Fig. 1). At the Mediterranean coastline most of the porous

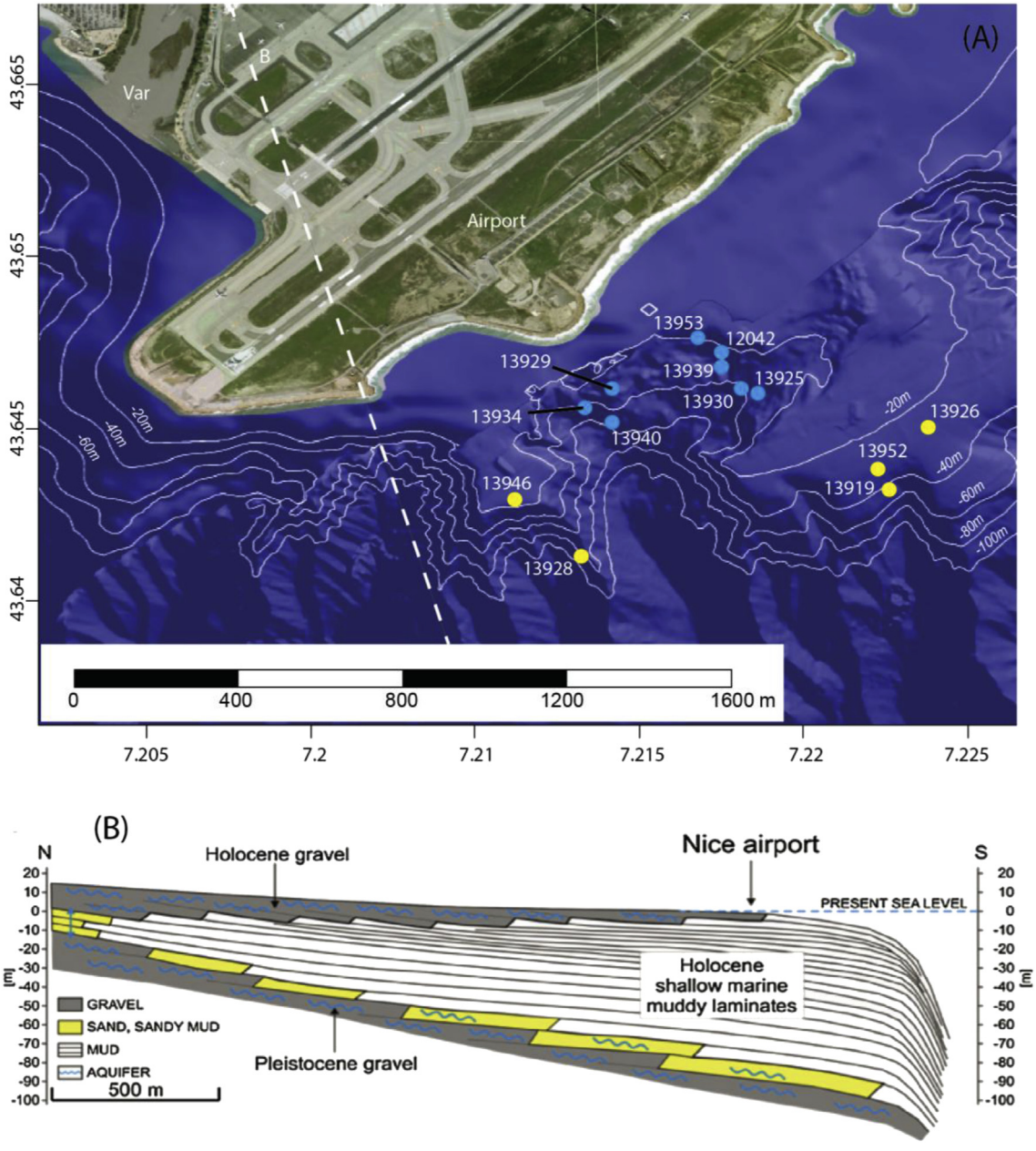


**Fig. 1.** (A) Bathymetric map of the study area south of the Nice airport. Gravity cores recovered from outside of the landslide scar (yellow) were only affected by seawater, while cores inside of the landslide scar (blue) were affected by submarine fresh groundwater. (B) Schematic cross section through the study area. The location is indicated in (A) by the white dotted line. Two aquifers systems, a lower confined and an upper unconfined aquifer which is examined in this study are known (modified after Dubar and Anthony (1995) and Kopf et al. (2016)). (For interpretation of the references to colour in this figure legend, the reader is referred to the web version of this article.)

coastal aquifers are located in Plio-Quarternary deposits (Lofi et al., 2012). The history of these aquifers is closely linked to the Messissinian Salinity Crisis, which exposed the margin of the Mediterranean Sea to subaerial erosion (Lofi et al., 2005) and created deep valleys, which were subsequently filled with Pliocene-Quarternary deposits (Lofi et al., 2003).

In the Var Paleo-Valley, conglomerates and marls were deposited at the base of the Pliocene, overlain by a 100 m thick wedge of Holocene alluvial sediments (Sultan et al., 2004). Two aquifer systems, recharged by the river Var and subsurface infiltration formed in this sediment succession (Guglielmi and Mudry, 1996; Anthony and Julian, 1997). The upper delta sediments of mixed grain sizes form an unconfined aquifer, which we examine in this study. The basal, coarse-grained Pliocene conglomerate (so called Puddingstones) constitutes a second aquifer, confined below a thick wedge of shallow marine deltaic mud. A hydrological model and a hydrochemical investigation indicates that the second aquifer layer drains seawards along permeable gently southward-dipping beds at various depths down to ~140 m (Guglielmi, 1993; Guglielmi and Mudry, 1996; Anthony and Julian, 1997). Fresh submarine groundwater discharge seems to occur within a distance of less than 1.5 km off the coast (Guglielmi and Prieur, 1997) and has been shown to be linked to high discharge (floods) at the river Var and flow through the aquifer (Stegmann et al., 2011).

A detailed hydrochemical characerization of surface and groundwaters in the Var Valley was conducted by Potot et al. (2012). Groundwater chemistry in the aquifers is mainly affected by water/rock interaction (Potot et al., 2012). Surface and alluvial groundwaters are dominated by Ca and $SO_4$. Barium concentrations range from 0.2 to 0.3 μM and ammonium concentrations are below detection in Var river water and alluvial groundwater (Potot et al., 2012). The mean oxygen isotopic signature of the Var river is −10.0‰ VSMOW (−11.4 to −8.5‰ VSMOW) and alluvial groundwaters range from −10.3 to −6.3‰ VSMOW (Potot et al. (2012).

Currently, the Var river basin is increasingly affected by anthropogenic activities such as urbanization. In the 1970s a deepening of the river Var channel led to salt water intrusion and increased risk of flood damage (Anthony and Julian, 1997). In 1979 a landslide occurred at the pro-delta of the Nice slope, which was likely caused by a combination of creep in sensitive clay sediments, loading by landfill material and embankement construction, and a pore pressure rise owing to precipitation (Dan et al., 2007). The landslide exposed freshwater charged sediments to seawater (Kopf et al., 2010) and its scar has been showing freshened pore waters on a number of repeated cruises over the past decade (Kopf et al., 2007, 2009).

## 3. Methods

### 3.1. Pore water and sediment sampling

For sediment and pore water analyses, 13 gravity cores were collected within the area of the airport landslide scar (Fig. 1) using the research vessels *RV Meteor* in summer 2007 and *RV Poseidon* in summer 2009. In the shallow waters off Nice 6 m long gravity cores were taken to prohibit the core from super penetration and losing surface sediments. This strategy proved to be successful since the most recent deposits were cored on all occasions (for details see Kopf et al. (2016)). All gravity cores were taken in plastic liners and cut into 1 m segments on deck. To prevent a warming of the sediments on board, the cores were immediately stored at a temperature of about 4 °C. The wet sediment was exposed by cutting a small 'window' in the plastic liner at an interval of 25 cm. Eh and pH were measured directly in the sediment using punch-in electrodes. Pore water was extracted with rhizons (pore size 0.1 μm) (Seeberg-Elverfeldt et al., 2005). Depending on the sediment porosity, the amount of pore water recovered ranged from 4 to 20 mL. Electric conductivity was measured using a conductivity probe. Ammonium was measured on board using a conductivity method (modified after Hall and Aller, 1992). Aliquots of the remaining pore water samples were diluted 1:10 and acidified with ultrapure $HNO_3$ for laboratory analyses at the University of Bremen. There, cation (Ca, Mg, Sr, K, Ba, S, Mn, Si, B, Li) concentrations were determined by ICP-OES, chloride and sulfate were measured with an ion chromatograph following established procedures (Price et al., 2007). Oxygen and hydrogen isotopes were measured using a "Liquid-Water Isotope Analyzer" (Los Gatos™). $\delta^{18}O$ and $\delta D$ are reported as deviations in permil (‰) from the Vienna Standard Mean Ocean Water (VSMOW).

Solid-phase samples of most cores were taken for total digestions, sequential extractions and mineralogical analyses at 25 cm intervals, and kept at 4 °C in gastight glass and heavy plastic bottles under an argon atmosphere.

The saturation index (SI) calculation for certain mineral phases (e.g. barite) was performed using the software PHREEQC (version: Phreeqc Interactive 3.2.0−9820 and the database llnl.dat, Lawrence Livermore National Laboratories) (Parkhurst and Appelo, 1999) for each depth interval in each core. The ion activity product and the solubility of all pore water species which are related to a certain mineral phase were considered. A negative SI (under saturation) indicates that, based on thermodynamic considerations, a given mineral should dissolve. Positive SI (over saturation) values indicate that a given mineral should precipitate within the pore water.

### 3.2. Pore water modelling

Assuming constant temperatures and porosities (in both time and depth), the distribution of chloride in sediment pore water is controlled by dispersion and advection according to the following equation (Berner, 1980).

$$\frac{\partial C}{\partial t} = v\frac{\partial C}{\partial x} - D_s\frac{\partial^2 C}{\partial x^2} \quad (1)$$

where $C$ is the concentration of chloride, $t$ is the time passed since the landslide occurred, $x$ is the depth below the seawater mixed sediment, $v$ is the advection rate, and $D_s$ is the chloride (hydrodynamic) dispersion coefficient. The $D_s$ term (in $cm^2\ s^{-1}$, Eq (2)) is composed of two parts. The chloride diffusion (first term in right hand side of Eq. (2)) was calculated for an average bottom water temperature ($T_c$) of 17 °C and corrected for tortuosity according to Boudreau (1997) as it acts within a sediment matrix (as represented by the denominator term). The second term on the right hand side represents the mechanical dispersion coefficient, which scales to pore-water velocity:

$$D_s = \frac{(9.6 + 0.438T_C)10^{-6}}{1 - 2\ln(\varnothing)} + \left|\alpha v\right| \quad (2)$$

where $\alpha$ is the dispersivity coefficient (= 10.0 cm), $T_C$ is the temperature in Celsius (=17 °C), and $\varnothing$ is the porosity. Values obtained for $D_s$ are dominated by molecular diffusion and range from 209 to 345 $cm^2\ yr^{-1}$ for the various porosity values. Eq. (1) has the following analytical solution (van Genuchten and Alves 1982).

$$C = (C_i + (C_0 - C_i))\left(0.5\mathrm{erfc}\left(\frac{x - vt}{2\sqrt{D_s t}}\right) + 0.5\exp\left(\frac{vx}{D_s}\right)\mathrm{erfc}\left(\frac{x + vt}{2\sqrt{D_s t}}\right)\right) \quad (3)$$

where $C_i$ is the initial chloride concentration in the freshwater portion of the sediment, and $C_0$ is the concentration at the top of the freshwater layer. In equation (1) the advection rate with respect to a fixed sediment layer ($v$) is the remaining unknown, as the diffusion coefficient in sediments is well constrained. Thus, $v$ can be obtained by comparing modeled chloride profiles with measured data and minimizing the sum of the least squares. A sensitivity analysis for the porosity, temperature and advective velocity is shown in supplementary materials.

## 4. Results

The gravity cores could generally be divided into two groups based on their position in the area of the Nice airport landslide scar. The first group refers to gravity cores recovered from adjacent areas of the 1979 landslide scar on the stable shelf/plateau (Fig. 1 marked in yellow). The second group consists of gravity cores taken in the 1979 landslide scar (Fig. 1 marked in blue).

### 4.1. Gravity cores outside the landslide scar

The most common deposit on the Nice Slope outside the 1979 landslide scar was a slightly plastic to medium plastic silty clay, mainly derived from the suspension load of the river Var (Kopf et al., 2016). The clays were often deformed by creep and flow processes or slump folding. In the fairly homogeneous package, thin (mm-to cm-thick) layers of silt or fine sand were also present.

The pore water composition of gravity cores collected outside of the landslide scar was dominated by seawater as indicated by major ion concentrations similar to Mediterranean Seawater (e.g. around 600 mM for chloride) (Figs. 2A and 2B). Sulfate concentrations decreased in each core from typical seawater concentrations in the range of 29 mM (Grasshoff et al., 2009) in the top section, to values below the detection limit (<1 μM) with depth. A zone with elevated pore water barium concentrations was observed in the deepest section of each core (about 3–4 m), which coincided with a zone where barite was under saturated, i.e., SI < 0. Pore water in the upper sections of the cores was over saturated with respect to barite, as indicated by a positive saturation index of barite (Figs. 2A and 2B).

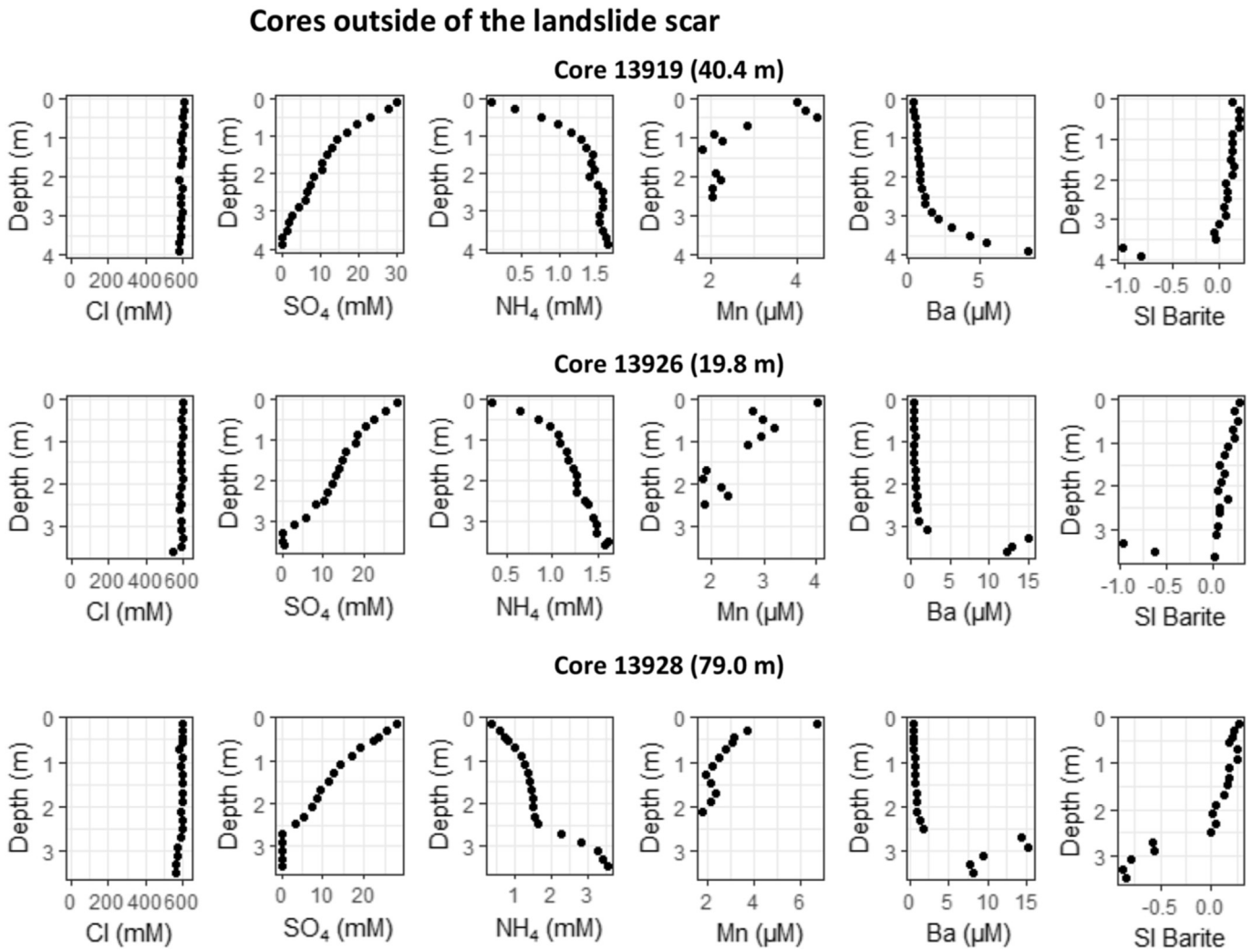


**Fig. 2A.** Pore water profiles (Cl, $SO_4$, $NH_4$, Mn, Ba and the saturation index of barite) of gravity cores which were collected outside of the landslide scar and were only affected by seawater. The water depth of each station is shown in brackets behind each station name.

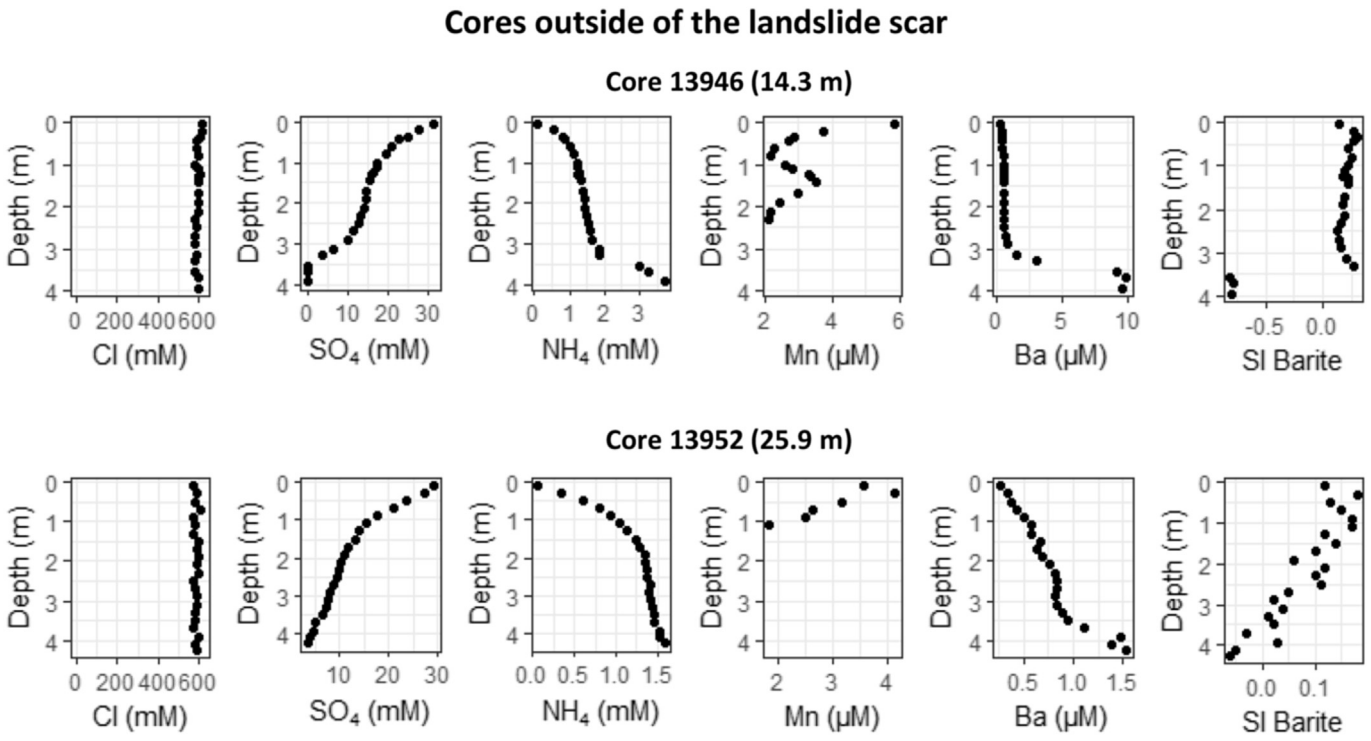


**Fig. 2B.** Pore water profiles (Cl, $SO_4$, $NH_4$, Mn, Ba and the saturation index of barite) of gravity cores which were collected outside of the landslide scar and were only affected by seawater. The water depth of each station is shown in brackets behind each station name.

### 4.2. Gravity cores inside the landslide scar

In cores from inside the landslide scar, mass wasting deposits, such as alluvial gravel and other coarse particles amalgamated into the clays of the Nice slope were common (Kopf et al., 2016). In places we found deposits that consist of the landslide debrite (e.g. core 13929), a deposit from the tsunami following the landslide (e.g. core 13953), and deposits out of a suspension cloud either from the tsunami or Var river discharge (e.g. core 13939).

Most pore water profiles from within the landslide scar can be divided into two zones. In the upper first meter of the sediment we observed a seawater dominated zone as indicated by comparatively high chloride concentrations. Below, we observed a second fresh to brackish groundwater affected zone indicated by lower chloride concentrations (Figs. 3A and 3B). Within this second brackish to freshwater affected zone, chloride concentrations decreased with sediment depth either in form of a concave shaped pore water profile (e.g. 13925, 13929, 13934, 13940, 12042) or a linear pore water profile (13939). Porewater profiles of other major ions of seawater (e.g. Li, Mg, K, Ca, Sr, Na) and $\delta^{18}O$ and $\delta D$ followed the chloride profile in a similar way (see electronic supplementary material).

Barium pore water concentrations were depleted within the upper seawater dominated zone (Figs. 3A and 3B). In most cores barium pore water concentrations of more than 15 µM were observed within a brackish water mixing zone directly below the seawater dominated zone. In the lower fresh groundwater dominated zone, barium pore water concentrations decreased with sediment depth down to concentrations of 0.3–1 µM in cores with a concave shaped chloride profile. Core 13939, which was dominated by a linear chloride profile (Fig. 3B), showed comparably higher pore water barium concentrations of 5 µM in the deeper part of the core.

Oxygen ($\delta^{18}O$) and hydrogen ($\delta D$) isotopes of pore waters from cores inside of the landslide scar are shown in Fig. 4. The most depleted values were −9.4‰ for $\delta^{18}O$ and −64‰ for $\delta D$. Values for seawater were in a positive range of up to +1.7‰ for $\delta^{18}O$ and +6.9‰ for $\delta D$, which is a typical value for Mediterranean seawater (Schmidt et al., 1999). The isotopes indicated linear mixing between meteoric water and seawater, which was mostly below the local meteoric water line (LMWL) (Fig. 4) and the global meteoric water line (GMWL) (Fig. 4). Endmember values of oxygen isotopes were calculated by applying a linear regression of pore water $\delta^{18}O$ values against pore water chloride concentrations for each respective core inside the landslide scar. Endmember values were in the range of −8.1 to −9.4‰ for $\delta^{18}O$ (Table 1 (D)), which was in a range similar to alluvial groundwater and Var river water sampled in the vicinity of the Var river mouth (Potot et al., 2012).

## 5. Discussion

### 5.1. Barium cycling in the subterranean estuary

Within the coastal area of the Nice airport, we observed a STE (after Moore, 1999) inside of the landslide scar, which most likely evolved after the landslide exposed fresh groundwater charged sediments to seawater (e.g. within 30 years prior to sampling). Outside of the landslide scar pore waters were only affected by seawater. We can thus directly compare barium cycling in pore waters which were affected and which were not affected by submarine fresh groundwater.

In sites which were only affected by seawater, the zone in which barium was released into the pore water coincided with a zone which was depleted in sulfate pore water concentrations and which was under saturated with respect to barite (Figs. 2A and 2B). In these sites, barium might be released into the pore water due to the dissolution of barite, forced by the depletion of sulfate within the zone of sulfate reduction (Henkel et al., 2012).

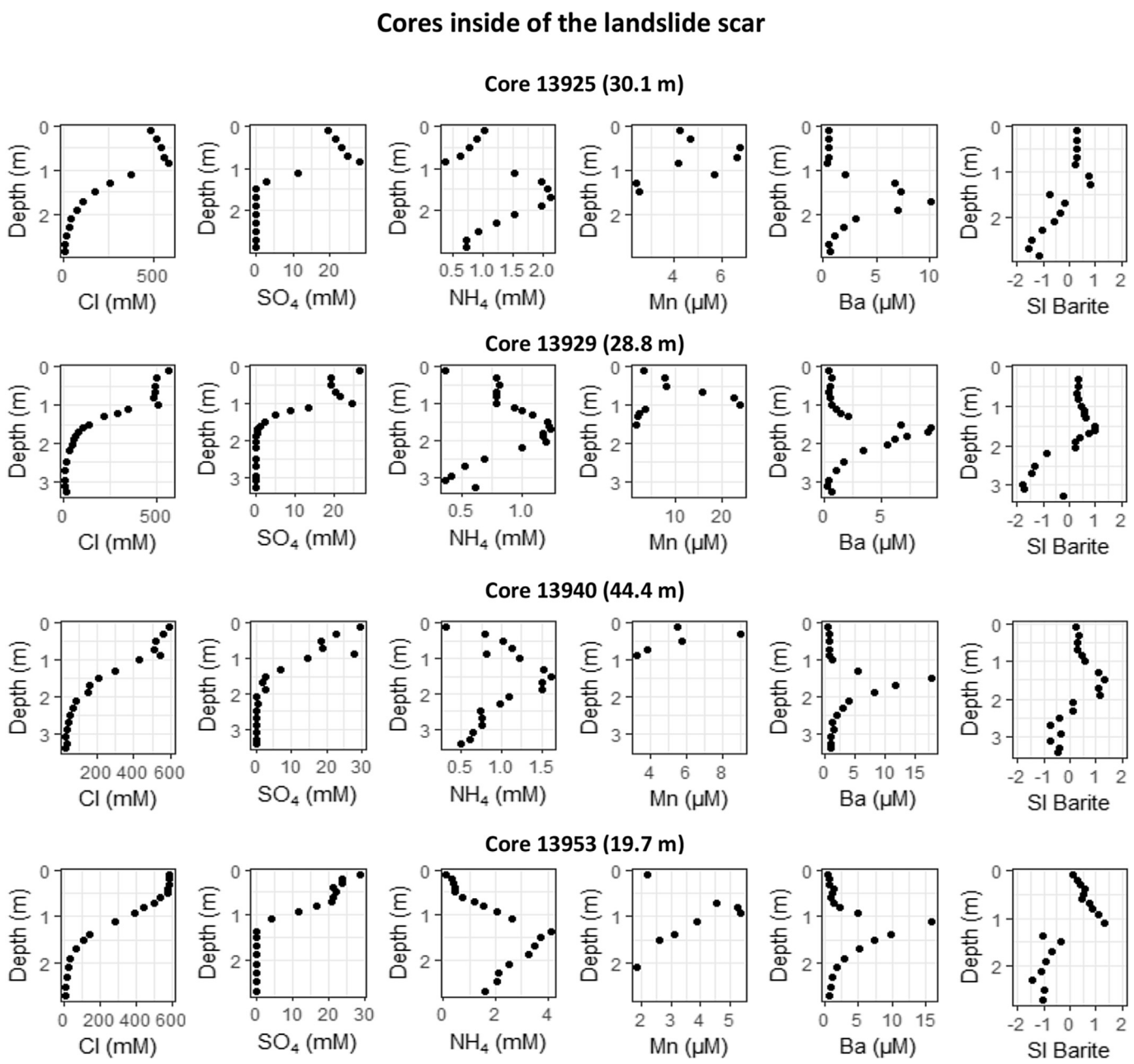


**Fig. 3A.** Pore water profiles (Cl, $SO_4$, $NH_4$, Mn, Ba and the saturation index of barite) of gravity cores which were collected inside the landslide scar. In most cores pore water profiles of chloride indicated the presence of seawater in the upper first meter of the sediment and an admixture of submarine fresh groundwater from below. The water depth of each station is shown in brackets behind each station name.

In fresh groundwater dominated sites, barium was released into the pore water within the brackish mixing zone, which was oversaturated with respect to barite (Figs. 3A and 3B). Barite dissolution as a source of barium seems unlikely, as solid phase barium concentrations did not show any significant variations with sediment depth (see electronic supplementary material). Similarly, because Mn pore water concentrations were depleted within the brackish water zone (Figs. 3A and 3B), a release of barium related to the dissolution Mn oxides (Charette and Sholkovitz, 2006) also appears unlikely. A remaining source of barium could be related to cation exchange reactions within the brackish water zone (Russak et al., 2016). This latter source is corroborated by pore water ammonium profiles, which are also strongly affected by cation exchange reactions (Russak et al., 2015) and closely follow the barium profile trends.

In most cores, barium freshwater endmembers in the deeper part of the core still exceeded those of Var river water or alluvial groundwater. If fresh groundwater in the landslide scar was derived from Var river water or alluvial groundwater as indicated by $\delta^{18}O$ values, a further barium source in the deeper part of the sediment must exist.

### 5.2. Submarine groundwater discharge within the landslide scar

The rate of vertical pore water advection within the sediments of the landslide scar can be calculated by modeling the pore water chloride profile (Fig. 5), assuming that before the landslide fresh groundwater was located in the deeper part of the sediment. If only

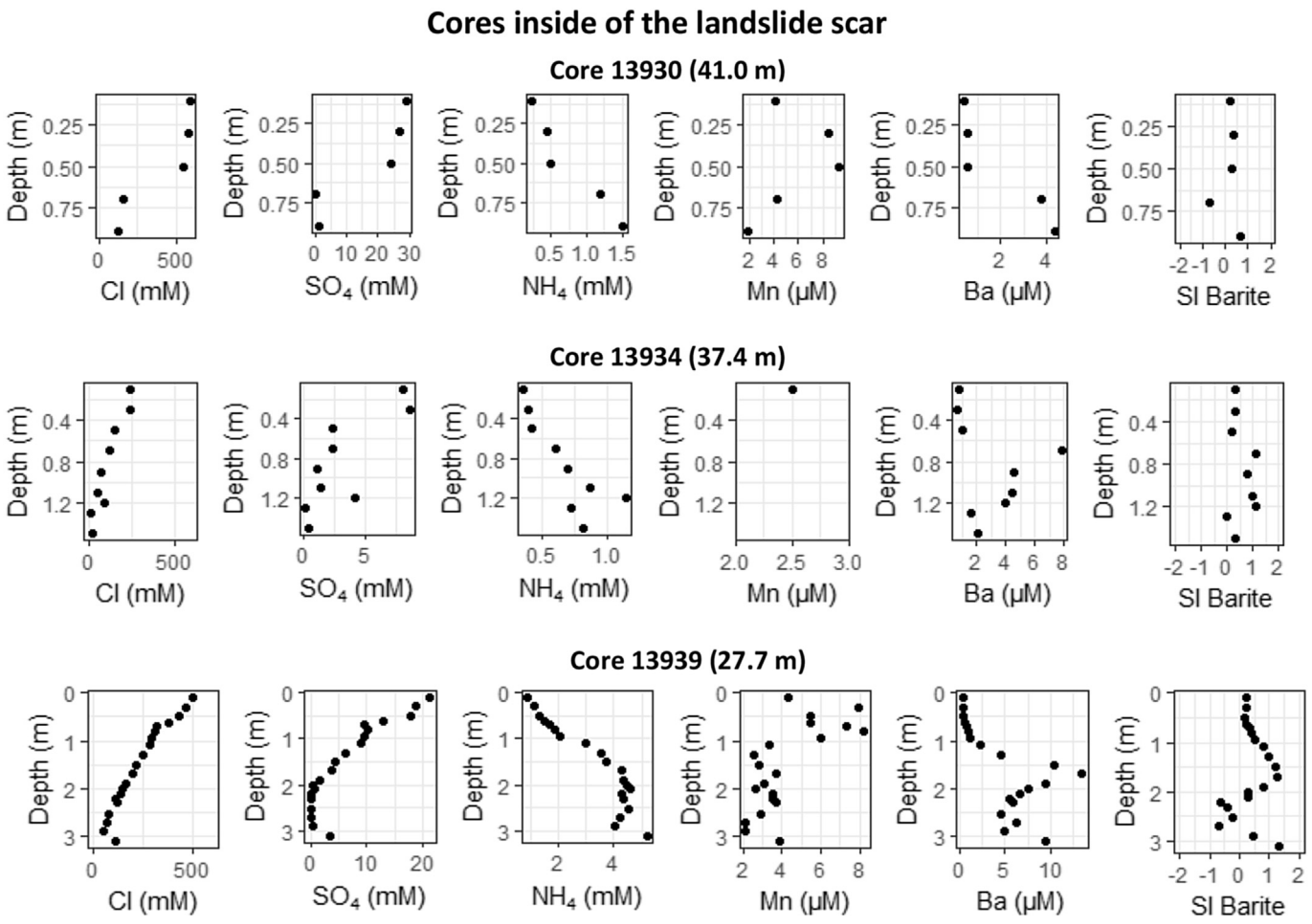


**Fig. 3B.** Pore water profiles (Cl, $SO_4$, $NH_4$, Mn, Ba and the saturation index of barite) of gravity cores which were collected inside the landslide scar. The water depth of each station is shown in brackets behind each station name. Also note the comparatively large amount of freshwater in core 13934 and core 13939 in top core sediments and the comparatively short penetration depth of core 13934 and 13930.

diffusion affected the mixing of groundwater with seawater, a curvature similar to the red dotted line, indicated in Fig. 5, would have developed after 30 years. Therefore, an upper mixed seawater zone, followed by a concave shaped chloride profile indicated either advective transport of freshwater from below or a change in chloride concentrations from above. A change in chloride concentrations from above could have been due to rapid sedimentation and burial, e.g. from the mass wasting after the 1979 landslide or sediment suspension of the Var river (Berner, 1980; Kopf et al., 2016) or due to seawater intrusion forced by differences in the hydraulic heads between land and sea, density driven transport and/or bottom water currents (Burnett et al., 2006; Santos et al., 2009).

Most of the modelled pore water profiles indicated an upward flow of freshwater (Table 1), which coincided with an upward migration of barium and ammonium poor fresh groundwater in cores with concave shaped chloride profiles (Figs. 3A and 3B). In one core (13939) seawater intrusion was indicated by the pore water model (Table 1), which coincided with comparatively high ammonium and barium concentrations in the deeper part of the core and thus no dilution by freshwater from below (Fig. 3B). While in most cores, fresh groundwater seemed to flow upwards it did not replace the upper seawater dominated layer, possibly because seawater was recirculating trough the upper, in general less compacted sediment layer. Intensive mixing processes from density driven seawater recirculation, rapid sediment deposition and resuspension, coupled to horizontal bottom-water currents penetrating (and possibly scouring) into this upper sediment layer might help to maintain near seawater concentrations. This mixing seems to be sufficiently strong to overcome the vertical fresh groundwater advection occurring within the landslide scar.

The 1-D advection-diffusion pore water model (eq. (1)) was applied to the concave and linear shaped part of the pore water profile. Calculated pore water velocities based on the advection-diffusion model yielded upward flow velocities of about +2.3 to +8.8 cm $yr^{-1}$ with an average upward flow velocity of +4.8 cm $yr^{-1}$. A volumetric discharge can be calculated by multiplying the pore water velocity with the porosity in each core, respectively. The volumetric discharge was in a range of 0.0124 $m^3$ $m^{-2}$ $yr^{-1}$ to 0.053 $m^3$ $m^{-2}$ $yr^{-1}$ with an average volumetric discharge of 0.026 $m^3$ $m^{-2}$ $yr^{-1}$.

SGD fluxes into the Mediterranean sea were mostly studied in karstic aquifers and are reported to be in the range of 37.6 $m^3$ $m^{-2}$ $yr^{-1}$ on the island of Majorca (Spain) (Basterretxea et al., 2010), 29.2 $m^3$ $m^{-2}$ $yr^{-1}$ total SGD and 18.2 $m^3$ $m^{-2}$ $yr^{-1}$ fresh SGD in Dor Bay (Israel) (Weinstein et al., 2007), 9.1 $m^3$ $m^{-2}$ $yr^{-1}$ fresh SGD in the Alcalfar cove on Minorca (Spain) (Garcia-Solsona et al., 2010a), 1.6–10 $m^3$ $m^{-2}$ $yr^{-1}$ total SGD in the Messiniakos Gulf (SE Ionian Sea) (Pavlidou et al., 2014). SGD fluxes in the sediments of the landslide scar were about 2–3 orders of magnitude lower

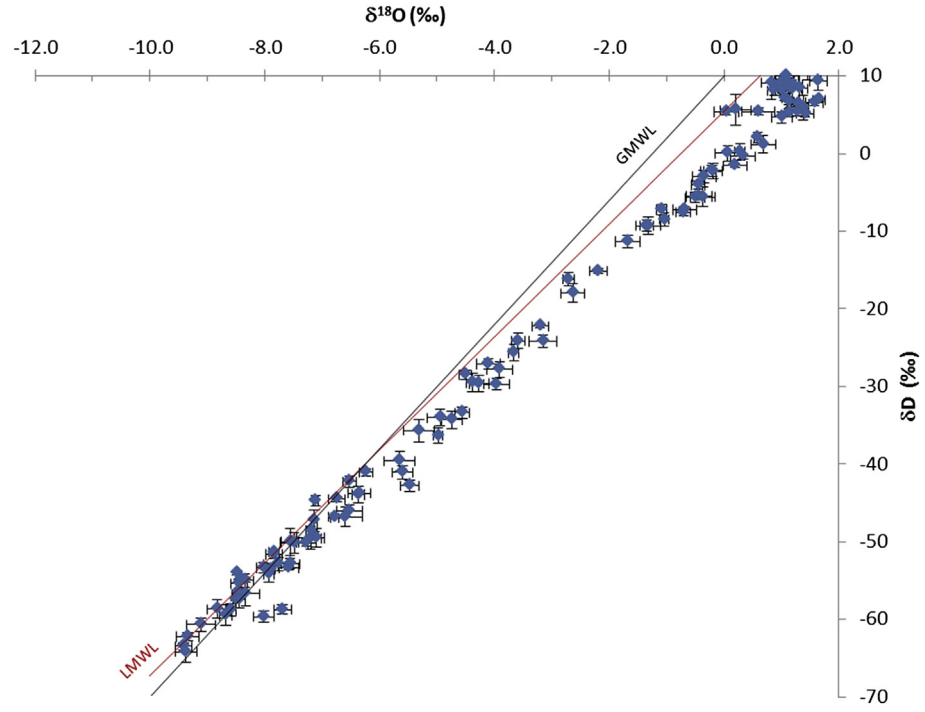


**Fig. 4.** $\delta^{18}O$ and $\delta D$ values of pore waters (blue dots) in the landslide scar. Error bars are shown by the black lines. A local meteoric water line which was collected from the nearby city of Genoa is shown by the red line (IAEA/WMO, 2017). The global meteoric water line is shown by the black line. (For interpretation of the references to colour in this figure legend, the reader is referred to the web version of this article.)

**Table 1**
Stations at which pore water samples were collected within the area of the landslide scar. Column (A) shows the name of the station. Column (B) indicates the water depth in meters in which the gravity cores were collected. (C) indicates the depth of the barium peak within each core. (D) shows freshwater normalized stable isotope endmembers of $\delta^{18}O$. (E) shows the dispersion coefficient, (F) the chloride concentration at the top of the freshwater layer and (G) the porosity used in the pore water model. In (H) the calculated pore water velocities (advection rates) from the pore water model are shown, with positive numbers showing an upward directed pore water flow and negative numbers showing a downward directed pore water flow.

| (A) Station | (B) water depth | (C) Barium peak | (D) $\delta^{18}O$ freshwater endmember | (E) Dispersion coefficient | (F) $C_0$ | (G) Porosity | (H) Pore water velocity | |
|---|---|---|---|---|---|---|---|---|
| | (m) | (m) | (‰) | ($cm^2/s$) | (mM) | (-) | (cm/yr) | |
| 13928 | 79 | 2.7 | - | - | - | - | - | *Outside of scar* |
| 13946 | 14.3 | 3.7 | - | - | - | - | - | |
| 13919 | 40.8 | 4 | - | - | - | - | - | |
| 13952 | 25.9 | - | - | - | - | - | - | |
| 13926 | 19.8 | 3.5 | - | - | - | - | - | |
| 13930 | 41 | - | -8.11 | - | - | - | - | *Inside of scar* |
| 13939 | 27.7 | 1.5 | -9 | 209 | 320 | 0.4 | -2.6 | |
| 13925 | 30.1 | 1.5 | -8.8 | 311 | 587 | 0.6 | +5.5 | |
| 13953 | 19.7 | 1 | -8.5 | 259 | 572 | 0.55 | +2.3 | |
| 13929 | 28.8 | 1.5 | -9.1 | 345 | 505 | 0.6 | +8.8 | |
| 13934 | 37.4 | - | -9.4 | 214 | 239 | 0.4 | +3.1 | |
| 13940 | 44.4 | 1.5 | -8.5 | 286 | 547 | 0.6 | +2.9 | |
| 12042 | 28.4 | - | - | 260 | 493 | 0.45 | +6.0 | |

compared to these fluxes, which might be attributed to slower groundwater seepage in sediments when compared to a karstic aquifer. Furthermore, the pore water model only considers the vertical component of SGD, whereas a large part of the pore water migration within the sediment may be horizontally. This is supported by the frequent silt bands and layers interbedded with the fine-grained muds (see Kopf et al., 2016), which may act as "conduits" for groundwater discharge.

## 6. Conclusions

In 1979, a submarine landslide next to the Nice airport (western Mediterranean Sea) exposed freshwater charged sediments to seawater. The distribution of dissolved chemical species (e.g. Cl, Ba, Mn, $NH_4$) in the pore water of the mixing zone between fresh groundwater and seawater indicated transport processes and reactions in the sediment. A 1-D advection-diffusion model estimated

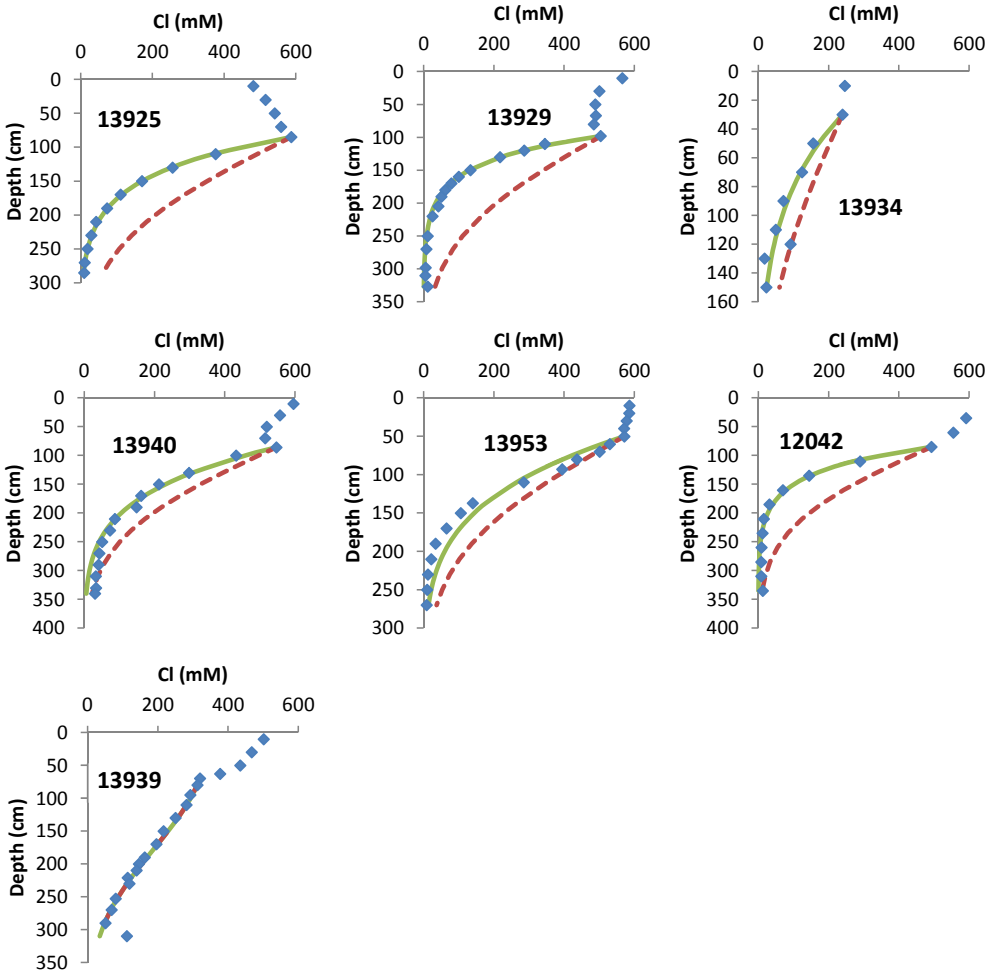


**Fig. 5.** Measured chloride profiles are shown in blue dots, modelled profiles according to an advection-diffusion model are shown in green lines and theoretical profiles which would have developed within 30 years due to diffusion only are shown in red dotted lines. (For interpretation of the references to colour in this figure legend, the reader is referred to the web version of this article.)

average vertical pore water velocities of 4.8 cm $yr^{-1}$ towards the sediment surface. In the Mediterranean Sea, it was recently shown that SGD derived nutrient fluxes can be on the same order of magnitude than river derived nutrient inputs (Rodellas et al., 2015), but submarine groundwater discharge has been studied mostly on karstic springs (Fleury et al., 2007; Bakalowicz, 2014). Our study indicates that submarine groundwater discharges also from sediments as deep as 44 m water depth. This might be an overlooked part of SGD especially along the French Mediterranean coastline.

## Acknowledgements

Deutsche Forschungsgemeinschaft is acknowledged for funding of slope stability research offshore Nice via MARUM Excellence Cluster (Grant FZT15/EXC309). Timo Fleischmann is acknowledged for providing the bathymetric map of the landslide scar. We thank two anonymous reviewers for their constructive comments.

## Appendix A. Supplementary data

Supplementary data related to this article can be found at http://dx.doi.org/10.1016/j.ecss.2017.09.006.

## References

Anthony, E., Julian, M., 1997. The 1979 Var Delta landslide on the French Riviera: a retrospective analysis. J. Coast. Res. 27–35.
Bakalowicz, M., 2014. Karst at depth below the sea level around the Mediterranean due to the Messinian crisis of salinity. Hydrogeological consequences and issues. Geol. Belg.
Basterretxea, G., Tovar-Sanchez, A., Beck, A.J., Masqué, P., Bokuniewicz, H.J., Coffey, R., Duarte, C.M., Garcia-Orellana, J., Garcia-Solsona, E., Martinez-Ribes, L., Vaquer-Sunyer, R., 2010. Submarine groundwater discharge to the coastal environment of a Mediterranean island (Majorca, Spain): ecosystem and biogeochemical significance. Ecosystems 13, 629–643.
Berner, R.A., 1980. Early Diagenesis: a Theoretical Approach, first ed. Princeton University press.
Boudreau, B.P., 1997. Diagenetic Models and Their Implementation. Springer, Berlin.
Burnett, W.C., Aggarwal, P.K., Aureli, A., Bokuniewicz, H., Cable, J.E., Charette, M.A., Kontar, E., Krupa, S., Kulkarni, K.M., Loveless, A., Moore, W.S., Oberdorfer, J.A., Oliveira, J., Ozyurt, N., Povinec, P., Privitera, A.M.G., Rajar, R., Ramessur, R.T., Scholten, J., Stieglitz, T., Taniguchi, M., V Turner, J., 2006. Quantifying submarine groundwater discharge in the coastal zone via multiple methods. Sci. Total Environ. 367, 498–543.
Burnett, W.C., Bokuniewicz, H., Huettel, M., Moore, W.S., Taniguchi, M., 2003. Groundwater and pore water inputs to the coastal zone. Biogeochemistry 66, 3–33.
Charette, M.A., Sholkovitz, E.R., 2006. Trace element cycling in a subterranean estuary: Part 2. Geochemistry of the pore water. Geochim. Cosmochim. Acta 70, 811–826.
Dan, G., Sultan, N., Savoye, B., 2007. The 1979 Nice harbour catastrophe revisited: trigger mechanism inferred from geotechnical measurements and numerical modelling. Mar. Geol. 245, 40–64.
Dörflinger, N., 2003. The state of the French Mediterranean coastal aquifers., p. 187–206. In: López-Geta, J.A., De Dios Gómez, J., De La Orden, J.A., Ramos, G.,

Rodríguez, L. (Eds.), The State of Seawater Intrusion in Mediterranean Countries.
Dubar, M., Anthony, E., 1995. Holocene environmental change and river-mouth sedimentation in the Baie des Anges, French Riviera. Quat. Res. 43, 329–343.
Elhatip, H., 2003. The use of hydrochemical techniques to estimate the discharge of Ovacık submarine springs on the Mediterranean coast of Turkey. Environ. Geol. 43, 714–719.
Fleury, P., Bakalowicz, M., de Marsily, G., 2007. Submarine springs and coastal karst aquifers: a review. J. Hydrol. 339, 79–92.
Froelich, P.N., Klinkhammer, G.P., Bender, M.L., Luedtke, N.A., Heath, G.R., Cullen, D., Dauphin, P., Hammond, D., Hartman, B., Maynard, V., 1979. Early oxidation of organic matter in pelagic sediments of the eastern equatorial Atlantic: suboxic diagenesis. Geochim. Cosmochim. Acta 43, 1075–1090.
Garcia-Solsona, E., Garcia-Orellana, J., Masqué, P., Garcés, E., Radakovitch, O., Mayer, A., Estradé, S., Basterretxea, G., 2010a. An assessment of karstic submarine groundwater and associated nutrient discharge to a Mediterranean coastal area (Balearic Islands, Spain) using radium isotopes. Biogeochemistry 97, 211–229.
Garcia-Solsona, E., Garcia-Orellana, J., Masqué, P., Rodellas, V., Mejías, M., Ballesteros, B., Domínguez, J.A., 2010b. Groundwater and nutrient discharge through karstic coastal springs (*Castelló*, Spain). Biogeosciences 7, 2625–2638.
van Genuchten, M.T., Alves, W.J., 1982. Analytical Solutions to the One-dimensional Convective-dispersive Solute Transport Equation. U.S. Departement of Agriculture.
Gilli, E., 2015. Deep speleological salt contamination in Mediterranean karst aquifers: perspectives for water supply. Environ. Earth Sci. 74, 101–113.
Grasshoff, K., Kremling, K., Ehrhardt, M., 2009. Methods of Seawater Analysis. John Wiley & Sons.
Guglielmi, Y., 1993. Hydrogéologie des aquifères Plio-Quaternaires de la Basse Vallée du Var.
Guglielmi, Y., Mudry, J., 1996. Estimation of spatial and temporal variability of recharge fluxes to an alluvial aquifer in a fore land area by water chemistry and isotopes. Ground Water 34, 1017–1023.
Guglielmi, Y., Prieur, L., 1997. Locating and estimating submarine freshwater discharge from an interstitial confined coastal aquifer by measurements at sea: example from the lower Var valley, France. J. Hydrol. 190, 111–122.
Hall, P., Aller, R., 1992. Rapid, small-volume, flow injection analysis for SCO2, and NH4+ in marine and freshwaters. Limnol. Oceanogr. 37, 1113–1119.
Henkel, S., Mogollón, J.M., Nöthen, K., Franke, C., Bogus, K., Robin, E., Bahr, A., Blumenberg, M., Pape, T., Seifert, R., März, C., de Lange, G.J., Kasten, S., 2012. Diagenetic barium cycling in Black Sea sediments – a case study for anoxic marine environments. Geochim. Cosmochim. Acta 88, 88–105.
IAEA/WMO, 2017. Global Network of Isotopes in Precipitation. The GNIP Database. Accessible at: http://www.iaea.org/water.
Kopf, A., Alexandrakis, J., Blees, J., Bogus, K., Dennielou, B., Förster, A., Girault, F., Haarmann, T., Hanff, H., Hentscher, M., Kaul, N., Klar, S., Krastel, S., Lange, M., Meier, M., Metzen, J., Spiess, V., Stegmann, S., Strozyk, F., Volen Krumova, T., 2007. Report and preliminary results of meteor cruise M73/1: Lima-Lamo (Ligurian margin landslide measurements and observatory). Berichte aus dem Fachbereich Geowiss. Univ. Brem. 264, 90–94.
Kopf, A.J., Stegmann, S., Garziglia, S., Henry, P., Dennielou, B., Haas, S., Weber, K.-C., 2016. Soft sediment deformation in the shallow submarine slope off Nice (France) as a result of a variably charged Pliocene aquifer and mass wasting processes. Sediment. Geol. http://dx.doi.org/10.1016/j.sedgeo.2016.05.014.
Kopf, A., Kasten, S., Blees, J., 2010. Geochemical evidence for groundwater-charging of slope sediments: the Nice airport 1979 landslide and tsunami revisited, p. 203–214. In: Submarine Mass Movements and Their Consequences. Springer, Netherlands.
Kopf, A., Blandin, A.R.J., Brulport, J., Crassous, P., Fleischmann, T., Förster, A., Guyader, G., Hammerschmidt, S., Henry, P., Jacinto Silva, R., Legrand, J., Mayer, A., Pape, S., Pelleau, P., Pichavant, P., Pichler, T., Price, R., Seydel, M., Stegmann, S., Weber, K., 2009. Report and preliminary results of poseidon cruise P386: NAIL (Nice Airport Landslide). Berichte aus dem Fachbereich Geowiss. Univ. Brem. 271, 88–96.
Lofi, J., Gorini, C., Berné, S., Clauzon, G., Tadeu Dos Reis, A., Ryan, W.B.F., Steckler, M.S., 2005. Erosional processes and paleo-environmental changes in the western Gulf of Lions (SW France) during the Messinian salinity crisis. Mar. Geol. 217, 1–30.
Lofi, J., Pezard, P., Bouchette, F., Raynal, O., Sabatier, P., Denchik, N., Levannier, A., Dezileau, L., Certain, R., 2012. Integrated onshore-offshore investigation of a Mediterranean layered coastal aquifer. Ground Water 51 no-no.
Lofi, J., Rabineau, M., Gorini, C., Berne, S., Clauzon, G., 2003. Plio–quaternary prograding clinoform wedges of the western Gulf of lion continental margin (NW Mediterranean) after the Messinian salinity crisis. Mar. Geol. 189 (3), 289–317.
Mogollón, J.M., Mewes, K., Kasten, S., 2016. Quantifying manganese and nitrogen cycle coupling in manganese-rich, organic carbon-starved marine sediments: examples from the Clarion-Clipperton fracture zone. Geophys. Res. Lett. 43, 7114–7123.
Moore, W., 1997. High fluxes of radium and barium from the mouth of the Ganges-Brahmaputra River during low river discharge suggest a large groundwater source. Earth Planet. Sci. Lett. 150, 141–150.
Moore, W.S., 1999. The subterranean estuary: a reaction zone of ground water and sea water. Mar. Chem. 65, 111–125.
Parkhurst, D., Appelo, C., 1999. User's Guide to PHREEQC (Version 2): a Computer Program for Speciation, Batch-reaction, One-dimensional Transport, and Inverse Geochemical Calculations, 312 pp.
Pavlidou, A., Papadopoulos, V.P., Hatzianestis, I., Simboura, N., Patiris, D., Tsabaris, C., 2014. Chemical inputs from a karstic submarine groundwater discharge (SGD) into an oligotrophic Mediterranean coastal area. Sci. Total Environ. 488, 1–13.
Potot, C., Féraud, G., Schärer, U., Barats, A., Durrieu, G., Le Poupon, C., Travi, Y., Simler, R., 2012. Groundwater and river baseline quality using major, trace elements, organic carbon and Sr–Pb–O isotopes in a Mediterranean catchment: the case of the Lower Var Valley (south-eastern France). J. Hydrol. 472, 126–147.
Povinec, P.P., Aggarwal, P.K., Aureli, A., Burnett, W.C., Kontar, E.A., Kulkarni, K.M., Moore, W.S., Rajar, R., Taniguchi, M., Comanducci, J.-F., Cusimano, G., Dulaiova, H., Gatto, L., Groening, M., Hauser, S., Levy-Palomo, I., Oregioni, B., Ozorovich, Y.R., Privitera, A.M.G., Schiavo, M.A., 2006. Characterisation of submarine groundwater discharge offshore south-eastern Sicily. J. Environ. Radioact. 89, 81–101.
Price, R., Amend, J., Pichler, T., 2007. Enhanced geochemical gradients in a marine shallow-water hydrothermal system: unusual arsenic speciation in horizontal and vertical pore water profiles. Appl. Geochem. 22 (12), 2595–2605.
Rodellas, V., Garcia-Orellana, J., Masqué, P., Feldman, M., Weinstein, Y., 2015. Submarine groundwater discharge as a major source of nutrients to the Mediterranean Sea. Proc. Natl. Acad. Sci. 112, 3926–3930.
Russak, A., Sivan, O., Herut, B., Lazar, B., Yechieli, Y., 2015. The effect of salinization and freshening events in coastal aquifers on nutrient characteristics as deduced from column experiments under aerobic and anaerobic conditions. J. Hydrol. 529, 1282–1292.
Russak, A., Sivan, O., Yechieli, Y., 2016. Trace elements (Li, B, Mn and Ba) as sensitive indicators for salinization and freshening events in coastal aquifers. Chem. Geol. 441, 35–46.
Santos, I.R., Burnett, W.C., Chanton, J., Dimova, N., Peterson, R.N., 2009. Land or ocean?: Assessing the driving forces of submarine groundwater discharge at a coastal site in the Gulf of Mexico. J. Geophys. Res. 114, C04012.
Santos, I.R., Burnett, W.C., Misra, S., Suryaputra, I.G.N.A., Chanton, J.P., Dittmar, T., Peterson, R.N., Swarzenski, P.W., 2011. Uranium and barium cycling in a salt wedge subterranean estuary: the influence of tidal pumping. Chem. Geol. 287, 114–123.
Schlüter, M., Sauter, E., Andersen, C., Dahlgaard, H., Dando, P., 2004. Spatial distribution and budget for submarine groundwater discharge in Eckernforde Bay (western Baltic sea). Limnol. Oceanogr. 49, 157–167.
Schmidt, G., Bigg, G., Rohling, E., 1999. Global Seawater Oxygen-18 Database, v1.21. .
Seeberg-Elverfeldt, J., Schlüter, M., Feseker, T., Kölling, M., 2005. Rhizon sampling of pore waters near the sediment/water interface of aquatic systems. Limnol. Oceanogr. Methods 3, 361–371.
Stegmann, S., Sultan, N., Kopf, A., Apprioual, R., Pelleau, P., 2011. Hydrogeology and its effect on slope stability along the coastal aquifer of Nice, France. Mar. Geol. 280, 168–181.
Sultan, N., Cochonat, P., Canals, M., Cattaneo, A., Dennielou, B., Haflidason, H., Laberg, J.S., Long, D., Mienert, J., Trincardi, F., Urgeles, R., Vorren, T.O., Wilson, C., 2004. Triggering mechanisms of slope instability processes and sediment failures on continental margins: a geotechnical approach. Mar. Geol. 213, 291–321.
Tsabaris, C., Anagnostou, M.N., Patiris, D.L., Nystuen, J.A., Eleftheriou, G., Dakladas, T., Papadopoulos, V., Prospathopoulos, A., Papadopoulos, A., Anagnostou, E.N., 2011. A marine groundwater spring in Stoupa, Greece: shallow water instrumentation comparing radon and ambient sound with discharge rate. Procedia Earth Planet. Sci. 4, 3–9.
Weinstein, Y., Burnett, W.C., Swarzenski, P.W., Shalem, Y., Yechieli, Y., Herut, B., 2007. Role of aquifer heterogeneity in fresh groundwater discharge and seawater recycling: an example from the Carmel coast. Isr. J. Geophys. Res. 112, C12016.